

## Reentrant-spin-glass state in $\text{Ni}_2\text{Mn}_{1.36}\text{Sn}_{0.64}$ shape-memory alloy

S. Chatterjee,<sup>1</sup> S. Giri,<sup>1</sup> S. K. De,<sup>2</sup> and S. Majumdar<sup>1,\*</sup>

<sup>1</sup>*Department of Solid State Physics and Center for Advanced Materials, Indian Association for the Cultivation of Science, 2A & B Raja S. C. Mullick Road, Jadavpur, Kolkata 700 032, India*

<sup>2</sup>*Department of Materials Science, Indian Association for the Cultivation of Science, 2A & B Raja S. C. Mullick Road, Jadavpur, Kolkata 700 032, India*

(Received 29 October 2008; revised manuscript received 26 December 2008; published 19 March 2009)

The ground-state properties of the ferromagnetic shape-memory alloy of nominal composition  $\text{Ni}_2\text{Mn}_{1.36}\text{Sn}_{0.64}$  have been studied by dc magnetization and ac susceptibility measurements. Like few other Ni-Mn based alloys, this sample exhibits exchange bias phenomenon. The observed exchange pinning was found to originate right from the temperature where a steplike anomaly is present in the zero-field-cooled magnetization data. The ac susceptibility study indicates the onset of spin-glass freezing near this steplike anomaly with clear frequency shift. The sample can be identified as a reentrant spin glass with both ferromagnetic and glassy phases coexisting together at low temperature at least in the field-cooled state. The result provides us with a comprehensive view to identify the magnetic character of various Ni-Mn-based shape-memory alloys with competing magnetic interactions.

DOI: 10.1103/PhysRevB.79.092410

PACS number(s): 75.50.Lk, 75.60.Nt, 75.47.Np

Recently  $\text{Ni}_2\text{Mn}_{1+x}\text{Z}_{1-x}$  ( $Z=\text{In, Sn, and Sb}$ ) based ferromagnetic shape-memory alloys (FSMAs) have attracted considerable attention due to their multifunctional properties, which include magnetic superelasticity, giant magnetoresistance, large inverse magnetocaloric effect, and magnetic memory effect.<sup>1-5</sup> The observed phenomena are primarily related to the magnetic field ( $H$ ) induced reverse transition across the martensitic transformation (MT).<sup>6</sup> The stoichiometric Heusler compositions ( $\text{Ni}_2\text{MnZ}$ ) are all ferromagnetic with the Curie point lying above room temperature. The excess Mn doping at the expense of  $Z$  atoms induces structural instability in the system leading to the ferromagnetic shape-memory effect. Short-range antiferromagnetic (AFM) interaction between the excess Mn (at the  $Z$  site) and the original Mn atoms has been predicted for the doped alloys.<sup>7,8</sup> Although, predominantly ferromagnetic (FM) character is present in the Mn-doped alloys with  $T_C$  around 300 K, the AFM correlation is evident from the gradual decrease in saturation moment with increasing amount of excess Mn.<sup>7,9</sup> Diffuse peaks observed in the powder neutron-diffraction data of Ni-Mn-Sn alloys indicate the existence of incipient AFM coupling.<sup>10</sup>

Evidently, the magnetic nature of the ground state of the alloys may not be very simple. A fascinating evidence for the complex ground state of the alloys is the recently observed exchange bias (EB) phenomenon in bulk samples.<sup>9,11,12</sup> EB is referred to the shift of the center of the magnetic hysteresis loop from the origin when the sample has been cooled from high temperature in presence of magnetic field.<sup>13</sup> The origin of EB is generally ascribed to the presence of FM and AFM interfacial couplings in a heterogeneous sample. EB has also been observed in materials having FM/spin-glass (SG) and FM/ferrimagnet interfaces<sup>14,15</sup> other than FM/AFM systems. However in all the cases, it is required that the ordering temperature ( $T_{\text{NF}}$ ) for the nonferromagnetic phase (may be AFM, SG, or ferrimagnet) should be lower than the ferromagnetic Curie point ( $T_C$ ). An interesting characteristics of EB in all  $\text{Ni}_2\text{Mn}_{1+x}\text{Z}_{1-x}$  alloys is that it vanishes above a certain temperature  $T_B$ , which coincides with the foot of a steplike anomaly observed in the zero-field-cooled magnetization versus temperature data.

In the context of EB, such a temperature is generally referred as the exchange bias blocking temperature with a value  $T_B \leq T_{\text{NF}}$ .

Although there are several reports on the observation of EB in Heusler-based shape-memory alloys, very little efforts have been given to understand the origin of the effect. Undoubtedly, EB confirms the presence of a nonferromagnetic phase in the otherwise FM alloy. In order to understand the nature of the ground state and the significance of  $T_B$ , we have investigated the magnetic properties of one of the alloys ( $\text{Ni}_2\text{Mn}_{1.36}\text{Sn}_{0.64}$ ) showing EB. A reentrant-spin-glass-type behavior with freezing temperature ( $T_f$ ) above  $T_B$  is evident from our study.

The polycrystalline samples were prepared by argon arc melting the constituent elements. The dc magnetization ( $M$ ) and the ac susceptibility ( $\chi_{\text{ac}}$ ) of the samples were measured by quantum design superconducting quantum interference device (SQUID) magnetometer [magnetic property measurement system (MPMS) 6, Ever-cool model] and commercial cryogen free vibrating sample magnetometer from Cryogenic Ltd., UK in the temperature ( $T$ ) range 5–300 K.

Figure 1 shows the  $M$  versus  $T$  data in zero-field-cooled heating (ZFCH) and field-cooled heating (FCH) sequences in presence of  $H=100$  Oe. The anomaly in the  $M(T)$  data around 140 K indicates the signature of MT,<sup>16</sup> which has been indicated by  $T_M$ . The steplike anomaly in the ZFCH data just below 80 K is observed in the sample (the foot of which is indicated by  $T_B$ ), which is the typical signature of EB blocking temperature reported in case of various  $\text{Ni}_2\text{Mn}_{1+x}\text{Z}_{1-x}$  alloys.

In order to ascertain the true magnetic character of the anomaly above  $T_B$ , we recorded some minor heating-cooling lines around the step. In this protocol, the sample was first zero field cooled down to 20 K. Then the magnetization was measured in presence of 100 Oe field by varying the sample temperature back and forth from different turning points (e.g.,  $q$ ,  $s$ , and  $u$ ). In other words, sample temperature was increased from 20 K to a certain temperature  $T_m$  ( $70 \leq T_m \leq 95$  K) and cooled back to 20 K. It was repeated for several values of  $T_m$ . These minor lines ( $qr$ - $rq$ ,  $st$ - $ts$ ,  $uv$ - $vu$ ,

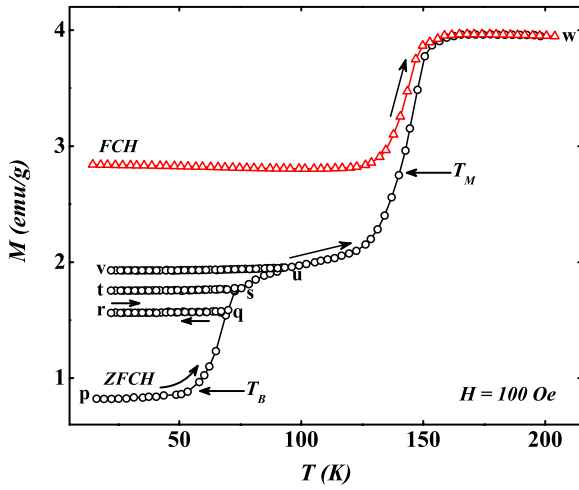


FIG. 1. (Color online) Magnetization is plotted as a function of temperature in ZFCH and FCH conditions in presence of 100 Oe of external magnetic field. The martensitic transformation and the EB blocking temperatures are indicated by  $T_M$  and  $T_B$  in the figure. Minor temperature cycling from a zero-field-cooled state above  $T_B$  are also shown in the figure (see text for details).

etc.) do not follow the master ZFCH curve ( $pqsu$ ), rather they trace different curves depending on the magnetization value at the turning point. Each individual minor curve does not show any thermal hysteresis, which one should not expect as we are well below the first-order MT. However, the present measurement indicates the signature of strong thermomagnetic irreversibility which exists locally around the steplike anomaly, and it might be the onset of some glassy magnetic phase in the system.

Now let us look at the EB behavior of the sample with respect to the different cooling fields ( $H_{cool}$ ) and  $M-H$  hysteresis loop temperatures ( $T_{MH}$ ). In the previous reports on EB, the  $M-H$  isotherms on the field-cooled and the zero-field-cooled states were recorded by cooling the sample from room temperature. Figure 2(a) shows such isotherms where sample was cooled from 300 K at different fields ( $H_{cool}=0, 0.5, \text{ and } 2.5$  kOe are only shown here for clarity). All the  $M-H$  loops were recorded between  $\pm 20$  kOe of fields; however, only a restricted region is depicted in Fig. 2 for clarity. The maximum field of 20 kOe is sufficient for the  $M-H$  isotherm to observe EB, as it is well above the technical saturation field of 7.5 kOe. A full loop is shown in the inset of Fig. 2(a) for completeness. The zero-field-cooled loop is perfectly symmetric with a rather soft FM character (coercive field  $\sim 250$  Oe), while field cooling makes it asymmetric with shift of the loop both in the field and the magnetization axes. The shift in the horizontal field axis ( $H_E$ ) and the vertical magnetization axis ( $M_E$ ) are plotted in Figs. 3(a) and 3(b) as a function of  $H_{cool}$  and  $T_{MH}$ , respectively.  $H_E$  increases with  $H_{cool}$  sharply at low field, attains a maximum for  $H_{cool} \approx 0.5$  kOe, and beyond that it decreases slowly with increasing  $H_{cool}$ . A considerable value of  $H_E$  (45 Oe) is observed for very low value of the cooling field ( $H_{cool} = 75$  Oe). On the other hand, EB decreases with increasing  $T_{MH}$ , and it almost vanishes at  $T_{MH} = 50$  K, which coincides with  $T_B$ , as defined in Fig. 1. This behavior is in line with the

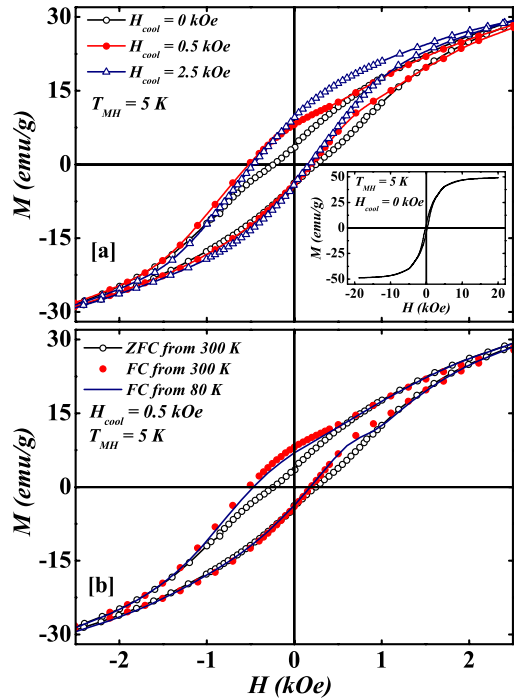


FIG. 2. (Color online) (a) Isothermal magnetization loops at 5 K after the sample being cooled in  $H=0, 0.5, \text{ and } 2.5$  kOe from 300 K. (b) Isothermal magnetization loops at 5 K after the sample being cooled in zero field, in 0.5 kOe from 300 K and in 0.5 kOe from 80 K. The magnetization loops were recorded by varying the field between  $\pm 20$  kOe, while data are shown here between  $\pm 2.5$  kOe for clarity. A full ( $\pm 20$  kOe) loop on the zero-field-cooled state is shown in the inset of (a).

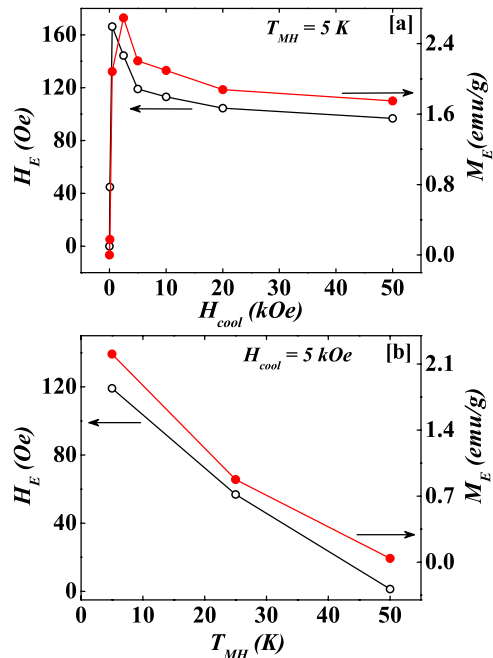


FIG. 3. (Color online) Exchange field ( $H_E$ ) and shift in magnetization ( $M_E$ ) are plotted (a) against the cooling field and (b) against the temperature of isothermal magnetization measurement.

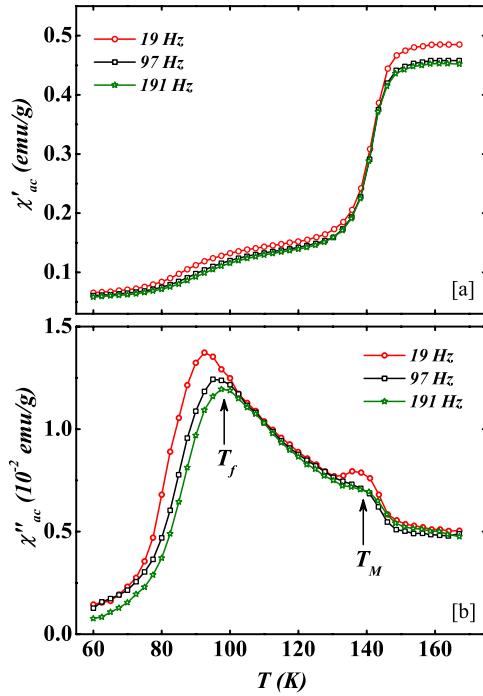


FIG. 4. (Color online) (a) Real part and (b) imaginary part of the ac susceptibility measured at different applied frequencies of the ac signal. The peak magnitude of the applied ac field is 10 Oe.

previous report of EB in different Ni-Mn-Z samples.

The most interesting observation is the  $T_{\text{cool}}$  (the temperature from where the sample is field cooled) dependence of the EB. We recorded EB by field cooling the sample from (i) 300 K, (ii) just above the steplike anomaly (80 K), and (iii) from below the steplike anomaly (40 K). In case of (ii) and (iii), the sample was zero-field-cooled from 300 to 80 K and 40 K, respectively, and then it was field cooled down to 5 K. There is practically no difference between the EB behavior for data taken by field cooling from 300 and 80 K. This has been shown in Fig. 2(b), where solid line and the filled circles loops almost coincide. Evidently, both the protocols show identical values of  $H_E$ . However when the sample was cooled from 40 K, no asymmetry in the  $M$ - $H$  loop was observed indicating  $H_E=0$ . The exchange pinning, therefore, actually takes place due to field cooling through the steplike anomaly, which is well below the martensitic transformation temperature. The anomaly signifies the second nonferromagnetic ordering below the  $T_C$ , and it is responsible for the EB in the sample.

Considering the fact that thermomagnetic irreversibility exists near the steplike anomaly, we performed ac susceptibility measurement at different frequencies to ascertain the existence of any spin-glass-like state. The ac susceptibility data are depicted in the temperature range 60–165 K, which covers the martensitic transformation temperature [indicated by  $T_M$  in Fig. 4(b)] and the steplike anomaly (above  $T_B$  in Fig. 1). Clear feature is visible in the real part ( $\chi'_{\text{ac}}$ ) as well as the out-of-phase part ( $\chi''_{\text{ac}}$ ) of the ac susceptibility data near the steplike anomaly. However, it is extremely prominent in  $\chi''_{\text{ac}}$ , where a broad peak is present. Strong feature in the out-of-phase component is an indication of the onset of

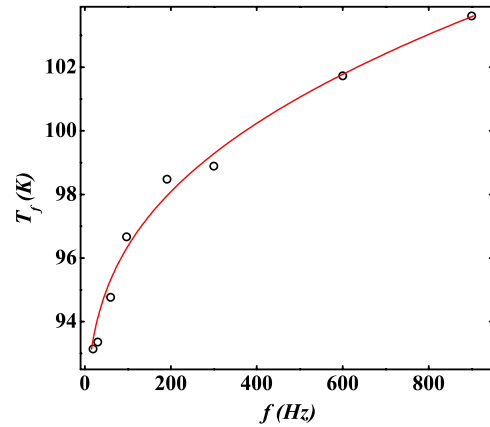


FIG. 5. (Color online) Frequency dependence of the peak in the imaginary part of the ac susceptibility observed near the steplike anomaly. The solid line is the Vogel-Fulcher fit to the data.

glassiness of the system. Interestingly, the feature near the steplike anomaly shows strong frequency ( $f$ ) dependence in both  $\chi'_{\text{ac}}$  and  $\chi''_{\text{ac}}$  data. This is the indication of a glassy magnetic state at low temperature. As expected, the first-order MT at  $T_M$  does not show any such  $f$  dependence and its signature in  $\chi'_{\text{ac}}$  is rather weak. Therefore, the frequency shift of the steplike anomaly is not directly linked to the metastability arising from the first-order MT. Figure 5 shows the frequency dependence of the peak temperature in  $\chi''_{\text{ac}}$  near the steplike anomaly [denoted by  $T_f$  in Fig. 4(b)]. The relative frequency shift is often expressed as  $\mathcal{P} = \Delta T_f / T_f (\Delta \log_{10} \omega)$ , where  $\omega$  is the angular frequency ( $\omega = 2\pi f$ ). For the present sample,  $\mathcal{P}$  was found to be 0.06, which lies well within the region of values for canonical spin glasses.<sup>17</sup> For spin glasses, empirical Vogel-Fulcher law,  $\omega = \omega_0 \exp[-E_a/k_B(T_f - T_0)]$ , is widely used to analyze the frequency dependence of  $T_f$ .<sup>17,18</sup> Here  $E_a$  is the activation energy of the spin glass,  $T_0$  is the Vogel-Fulcher temperature, and  $\omega_0$  is the characteristic frequency for spin freezing. The freezing temperature  $T_f(\omega)$  is the peak temperature of  $\chi''_{\text{ac}}$ , which lies at the onset point of the steplike anomaly in the dc magnetization. The Vogel-Fulcher fitting of the data has been shown by a solid line in Fig. 5. The fitted parameters,  $E_a$ ,  $\omega_0$ , and  $T_0$ , were found to be 100.9 K,  $5 \times 10^5$  Hz, and 81.5 K, respectively.

From the ac susceptibility analysis, it is clear that the sample show SG-like behavior with a frequency-dependent glassy transition above  $T_B$ . This is a remarkable example of glassy magnetic ground state for the “ferromagnetic” shape-memory alloy. The SG state is not of a conventional type, rather it has a reentrant character, where the sample first orders ferromagnetically from a paramagnetic state below  $T_C=330$  K and below a temperature  $T_f$  near the steplike anomaly, the sample further transforms from the ordered FM to a disordered glassy magnetic phase. Reentrant-spin-glass (RSG) behavior has been observed in variety of magnetic systems including metallic alloys and oxides.<sup>19–21</sup> We observe that the low-temperature nonferromagnetic ordering/freezing in the system responsible for the EB occurs around the steplike anomaly, and *field cooling from this temperature is sufficient enough to obtain the desired field shift* in the

isothermal magnetization measurements. The spin-glass-like freezing at  $T_f$  is actually responsible for the exchange pinning of the ferromagnetic moments, and we can identify  $T_{NF}$  to be  $T_f$ .

It appears that the MT at  $T_M$  does not have a direct role for the observed EB. It has been argued for Ni-Mn-based shape-memory alloys that short-range AFM correlation actually develops and/or becomes stronger below the MT.<sup>7,8,10</sup> Therefore, MT definitely plays a crucial role toward the spin freezing. Possibly, the diffuse AFM phase starts to develop below  $T_M$ , however, only at  $T_B$  it becomes strong enough to cause the spin freezing and subsequent pinning for the observed EB. Similar effect has been observed in case of Cr-doped manganites, where the actual spin freezing takes place well below the AFM ordering temperature.<sup>20</sup>

The observed RSG phase develops from spin frustration arising from the short-range AFM interaction which prevails between the excess Mn and the original Mn atoms in  $\text{Ni}_2\text{Mn}_{1+x}\text{Z}_{1-x}$  alloys. The steplike anomaly in the ZFC data is due to the drop in  $M$  arising from the random spin freezing. It is now pertinent to know the nature of the RSG phase, i.e., whether the ground state has a true SG character or both FM and SG coexists below  $T_f$ . The sample shows FM nature at low temperature in the FC state (see Fig. 1), and in addition, the observed EB for  $H_{\text{cool}}$  as low as 75 Oe indicates that FM and SG phases indeed coexists at 5 K for sample cooled in presence of low magnetic field. Coexistence of SG and FM phases is not unusual for RSG,<sup>19,22,23</sup> and several theo-

retical models predict that FM phase exists below the RSG transition (see, for example, Ref. 24, and references therein). Notably, in contrary to the conventional spin glasses, the peak magnitude at  $T_f$  in  $\chi''_{\text{ac}}$  of the present sample decreases with increasing  $f$ . Similar anomalous change in the peak magnitude has been observed in case of phase separated manganites.<sup>25</sup> However, from magnetization measurement only, it is difficult to comment on the coexistence of FM and SG phases in the sample. A more detailed studies, preferably based on neutron-scattering measurements can actually unveil the true ground-state characteristics of the sample.

In conclusion, we observe RSG behavior in the ferromagnetic shape-memory alloy of composition  $\text{Ni}_2\text{Mn}_{1.36}\text{Sn}_{0.64}$ . The spin-glass transition was found to be responsible for the observed EB phenomenon in the alloy. We would like to add that the very similar RSG phase and associated EB were also observed in the alloy  $\text{Ni}_2\text{Mn}_{1.44}\text{Sn}_{0.56}$ , which has a slightly higher Mn concentration. This second composition also shows frequency dependence in  $\chi_{\text{ac}}$  near the steplike anomaly although  $T_f$  has a much higher value (140 K). This prompts us to propose a generic view of the RSG-type magnetic ground state of various  $\text{Ni}_2\text{Mn}_{1+x}\text{Z}_{1-x}$ -type FSMAs showing EB, where a common spin freezing phenomena is responsible for the observed exchange bias in all these alloys.

The present work was financially supported by a grant from CSIR, India.

\*sspsm2@iacs.res.in

<sup>1</sup>R. Kainuma, Y. Imano, W. Ito, Y. Sutou, H. Morito, S. Okaoto, O. Kitakami, K. Oikawa, A. Fujita, T. Kanomata, and K. Ishida, *Nature (London)* **439**, 957 (2006).

<sup>2</sup>T. Krenke, E. Duman, M. Acet, E. F. Wassermann, X. Moya, L. Mañosa, and A. Planes, *Nature Mater.* **4**, 450 (2005).

<sup>3</sup>R. Kainuma, K. Oikawa, W. Ito, Y. Sutou, T. Kanomata, and K. Ishida, *J. Mater. Chem.* **18**, 1837 (2008).

<sup>4</sup>L. Mañosa, X. Moya, A. Planes, T. Krenke, M. Acet, and E. F. Wassermann, *Mater. Sci. Eng., A* **481-482**, 49 (2008).

<sup>5</sup>S. Chatterjee, S. Giri, S. Majumdar, and S. K. De, *Phys. Rev. B* **77**, 012404 (2008).

<sup>6</sup>K. Koyama, K. Watanabe, T. Kanomata, R. Kainuma, K. Oikawa, and K. Ishida, *Appl. Phys. Lett.* **88**, 132505 (2006).

<sup>7</sup>J. Enkovaara, O. Heczko, A. Ayuela, and R. M. Nieminen, *Phys. Rev. B* **67**, 212405 (2003).

<sup>8</sup>T. Krenke, E. Duman, M. Acet, E. F. Wassermann, X. Moya, L. Mañosa, A. Planes, E. Suard, and B. Ouladdiaf, *Phys. Rev. B* **75**, 104414 (2007).

<sup>9</sup>M. Khan, I. Dubenko, S. Stadler, and N. Ali, *Appl. Phys. Lett.* **91**, 072510 (2007).

<sup>10</sup>P. J. Brown, A. P. Gandy, K. Ishida, R. Kainuma, T. Kanomata, K. U. Neumann, K. Oikawa, B. Ouladdiaf, and K. R. A. Ziebeck, *J. Phys.: Condens. Matter* **18**, 2249 (2006).

<sup>11</sup>M. Khan, I. Dubenko, S. Stadler, and N. Ali, *J. Appl. Phys.* **102**, 113914 (2007).

<sup>12</sup>Z. Li, C. Jing, J. Chen, S. Yuan, S. Cao, and J. Zhang, *Appl.*

*Phys. Lett.* **91**, 112505 (2007).

<sup>13</sup>J. Nogués and I. K. Schuller, *J. Magn. Magn. Mater.* **192**, 203 (1999).

<sup>14</sup>M. Ali, P. Adie, C. H. Marrows, D. Greig, B. J. Hicky, and R. L. Stamps, *Nature Mater.* **6**, 70 (2007).

<sup>15</sup>M. Patra, K. De, S. Majumdar, and S. Giri, *Eur. Phys. J. B* **58**, 367 (2007).

<sup>16</sup>S. Chatterjee, S. Giri, S. Majumdar, and S. K. De, *Phys. Rev. B* **77**, 224440 (2008).

<sup>17</sup>J. A. Mydosh, *Spin Glasses: An Experimental Introduction* (Taylor & Francis, London, 1993).

<sup>18</sup>K. Binder and A. P. Young, *Rev. Mod. Phys.* **58**, 801 (1986).

<sup>19</sup>B. H. Verbeek, G. J. Nieuwenhuys, H. Stocker, and J. A. Mydosh, *Phys. Rev. Lett.* **40**, 586 (1978); M. Hennion, B. Hennion, I. Mirebeau, and S. Lequien, *J. Appl. Phys.* **63**, 4071 (1988).

<sup>20</sup>J. Dho, W. S. Kim, and N. H. Hur, *Phys. Rev. Lett.* **89**, 027202 (2002).

<sup>21</sup>R. Mathieu, P. Svedlindh, and P. Nordblad, *Europhys. Lett.* **52**, 441 (2000).

<sup>22</sup>S. Cao, W. Li, J. Zhang, B. Kang, T. Gao, and C. Jing, *J. Appl. Phys.* **102**, 053909 (2007).

<sup>23</sup>W. Bao, S. Raymond, S. M. Shapiro, K. Motoya, B. Fåk, and R. W. Erwin, *Phys. Rev. Lett.* **82**, 4711 (1999).

<sup>24</sup>T. H. Kim, M. C. Cadeville, A. Dinia, and H. Rakoto, *Phys. Rev. B* **53**, 221 (1996).

<sup>25</sup>I. G. Deac, J. F. Mitchell, and P. Schiffer, *Phys. Rev. B* **63**, 172408 (2001).